DALTON
FULL PAPER

Co-ordination of thorium(IV) in molten alkali-metal chlorides and the structure of liquid and glassy thorium(IV) chloride

G. M. Photiadis and G. N. Papatheodorou *

Institute of Chemical Engineering and High Temperature Chemical Processes - FORTH and Department of Chemical Engineering, University of Patras, PO Box 1414, GR-26500, Patras, Greece. E-mail: gpap@iceht.forth.gr

Received 24th June 1999, Accepted 31st August 1999

Raman spectra of molten $ThCl_4$–ACl (A = Li, Na, K or Cs) mixtures have been measured. The complete composition range has been studied for all systems at temperatures up to 960 °C. The spectral changes upon melting the binary compounds A_2ThCl_6, A_3ThCl_7 and the pure crystalline $ThCl_4$ were also measured. The data indicate that in molten mixtures rich in alkali-metal chloride the predominant species are the $ThCl_6^{2-}$ octahedra [$\nu_1(A_{1g})$ 297 and $\nu_5(F_{2g})$ 125 cm^{-1}] in equilibrium with the $ThCl_7^{3-}$ pentagonal bipyramid. With increasing $ThCl_4$ mole fraction above 0.3 the frequency of the $\nu_1(A_{1g})$ band increases continuously reaching its maximum (≈340 cm^{-1}) in pure molten $ThCl_4$. It appears that in mixtures rich in $ThCl_4$ edge bridging of thorium(IV) octahedra occurs yielding chain species of the type $[Th_nCl_{4n+2}]^{2-}$ and $[Th_nCl_{4n-2}]^{2+}$ where the end Th atoms of the chain are six- and four-fold co-ordinated for the anion and cation respectively. The known ionic character of these melts suggests that the chain length is rather small and that most probably the species have low n values (*e.g.* $Th_2Cl_{10}^{2-}$, $Th_3Cl_{14}^{2-}$, $Th_3Cl_{10}^{2+}$, . . .). Glassy $ThCl_4$ was formed by slow cooling of the melt. The vibrational modes and the inferred structure of the glass are similar to those of the melt.

Introduction

Recently we have used Raman spectroscopy to investigate the structural properties of molten $ZrCl_4$ and its binary mixtures with alkali-metal chlorides (CsCl).[1] It was found that in mixtures rich in alkali-metal chloride the predominant zirconium species present are the $ZrCl_6^{2-}$ octahedra. As the $ZrCl_4$ mole fraction increases other zirconium chloroanions ($Zr_2Cl_9^-$, $Zr_2Cl_{10}^{2-}/ZrCl_5^-$) are formed. At high $ZrCl_4$ mole fractions an equilibrium exists between $Zr_2Cl_9^-$ and monomeric and/or polymer-like $(ZrCl_4)_n$ species. The structure of pure molten $ZrCl_4$ is also described with an equilibrium molecular mixture of $ZrCl_4$ monomers and $(ZnCl_4)_n$ oligomers (n = 2 or 6). The large volume expansion upon melting $ZrCl_4$ and the formation of a high fluidity, non-conducting liquid are compatible with the suggested molecular character.

Structural studies of similar systems involving tetravalent metal halides are very few. This is in contrast to numerous studies involving divalent and trivalent systems where the structural systematics of the molten mixtures with alkali-metal halides and of the pure component salt have been derived.[2,3] The purpose of the present work is to investigate the structural properties of molten thorium(IV) chloride and its binary mixtures with alkali-metal chlorides (A = Li, Na, K or Cs). Thorium(IV) has relative to zirconium(IV) a higher ionic radius ($r_{Th^{4+}}$ = 0.95; $r_{Zr^{4+}}$ = 0.72 Å) and thus different structural properties may be expected in the corresponding molten chlorides and their mixtures with alkali-metal chlorides.

The electrical conductivity[4,5] of molten $ThCl_4$ appears to be ionic suggesting that the liquid structure is rather different from that of the molecular $ZrCl_4$ and TiX_4 (X = Cl, Br or I)[2,6] liquids. The phase diagrams of the $ThCl_4$–ACl (A = Li to Cs)[7,8] binaries show the formation of solid compounds with stoichiometries ATh_3Cl_{13} (A = Cs), $ATh Cl_5$ (A = Cs, Rb, K or Na), A_2ThCl_6 (A = Cs, Rb or K), A_3ThCl_7 (A = Cs, Rb or K) and A_4ThCl_8 (A = Li). The most stable compounds appear to be the A_3ThCl_7 having congruent melting points close to that of $ThCl_4$ (≈750 °C). Density,[9,10] viscosity,[11] electrical conductivity[4,5] and emf[12,13] measurements of molten $ThCl_4$–ACl binary systems have shown that deviation of the additive properties from ideality occurs at $ThCl_4$ mole fractions $X_{ThCl_4} \approx 0.33$. This behavior was attributed to the formation of $ThCl_6^{2-}$ complex ions in these melts. Vapor pressure measurements[14] over the $ThCl_4$–ACl molten mixtures show negative deviations from Raoult's law indicative of growing complexation of the thorium ions in these melts which increases in the sequence from LiCl to CsCl.

In contrast to the above findings, Raman spectra of the $ThCl_4$–KCl molten mixtures were interpreted as showing the presence of $ThCl_7^{3-}$ and $ThCl_5^-$ complexes while tetrahedral molecules were argued to exist in pure molten $ThCl_4$.[15,16] The existence of eight- and seven-co-ordinated thorium(IV) ions (*i.e.* ThF_8^{4-}, ThF_7^{3-}) in molten ternary ThF_4–LiF–NaF mixtures has also been deduced by Raman spectroscopy.[17]

The work reported here includes measurements of temperature and composition effects on the Raman spectra of all the $ThCl_4$–ACl (A = Li, Na, K or Cs) binary melts as well as of the spectral changes occurring upon heating and melting crystalline binary compounds formed in these binaries. The data are used to identify the different structural units present in the melt mixtures and in pure $ThCl_4$. Evidence is given for the formation of an all chloride seven-co-ordinated thorium complex.

Finally, from an applied point of view, the knowledge of the physicochemical properties of the $ThCl_4$–ACl melts is considered important due to the potential use of molten chlorides for the electrolytic production and/or refining of metallic thorium.[18]

Experimental

Thorium tetrachloride (Cerac 99.9%) was initially dried under vacuum (≈0.05 Torr) by slowly raising the temperature (T < 200 °C) for a few hours. Subsequent sublimation in high vacuum (≈10^{-6} Torr) at 630 °C produced a white material. This was doubly sublimed under static vacuum (≈0.05 Torr) to give high purity crystals of $ThCl_4$. Sublimation in high vacuum

(≈10^{-6} Torr) was also applied for the purification of LiCl (Merck 99.5%) and CsCl (Cerac 99.9%) at 700 °C. Solid NaCl and KCl (Merck 99.5%) were dried in mild vacuum (0.01 Torr) by gradually raising the temperature to 200 °C and finally melted under an argon atmosphere.

The moisture and oxygen sensitive chemicals ($ThCl_4$ is especially hygroscopic) were handled in a controlled nitrogen atmosphere dry-box (water content < 1 ppm) or in sealed glass tubes. Raman cells were made of fused silica tubes (3 mm i.d., 4 mm o.d. and ≈3 cm length) and loaded with approximately 200 mg of chemicals. Extended heating of cells having mixtures rich in $ThCl_4$ or pure $ThCl_4$ leads after 5–10 min to bleary cell walls. Thus, it was necessary to mix the salts in the cell rather rapidly and to use them only once for spectral measurements.

The Raman set-up including the optical furnace to obtain high-temperature quantitative spectra was the same as before.[1,19] Samples were illuminated with the lines of an Ar^+ laser. The spectra of melts were recorded in a 90° geometry using two polarization configurations of the incident-scattered light, the horizontal (HV) and the vertical (VV). A time of 4–5 min was required for the spectral measurements. Polycrystalline solids were measured using the unpolarized vertical (U-V) configuration. For measurements of the spectra of molten $ThCl_4$ at temperatures above 800 °C a Raman spectroscopic system equipped with a CCD detector[19a] was used giving the possibility for completing the accumulated spectra runs in ≈20 s. Within this time the reaction (corrosion) of $ThCl_4$ with the fused silica cell did not influence the spectra.

Over seventy Raman cells having different compositions were prepared and the spectra measured and stored digitally in a PC. For all measurements identical light-scattering optical geometries, laser intensities and size of cells were used; this permitted an error of much less than 5% in relative intensity measurements from different cells having a variety of melt composition.

Results and discussion

A large number of spectra were recorded for (a) the liquid mixtures listed in Table 1 and (b) all the solid compounds (incongruently or congruently melting) in the phase diagrams of $ThCl_4$–ACl (A = Li, Na, K or Cs). For each melt mixture spectra were measured from the liquidus temperature up to 800 °C. The solid spectra were measured from liquid nitrogen temperatures throughout the melting and up to 800 °C. Pure molten $ThCl_4$ was measured up to 960 °C. Only a limited number of spectra are presented here with emphasis on the CsCl containing melts. Detailed spectral figures and tables of frequencies at different temperatures of the solids and melts can be found elsewhere.[20] The discussion and the conclusion regarding the systematics of the liquid structure is extended to all melts studied.

Changes of vibrational modes upon melting Cs_2ThCl_6 and Cs_3ThCl_7

Cs_2ThCl_6. The crystal structure of Cs_2ThCl_6 has a trigonal $P\bar{3}m1$ (D^3_{3d}) symmetry and is isostructural to K_2GeF_6[8,21] and to all Cs_2AnCl_6 (An = Th to Pu)[22] compounds. Each thorium atom has a D_{3d} site symmetry surrounded by six chlorine atoms located at the corners of a slightly distorted $ThCl_6^{2-}$ octahedron. The distribution of vibrational modes is given in Table 2. Seven Raman active modes are expected but only six are seen in the lower temperature spectra presented in Fig. 1A. The seventh mode is a librational E_g mode that lies close to the Rayleigh wing and thus is not seen in the spectra. According to the $ThCl_4$–CsCl phase diagram,[8] Cs_2ThCl_6 melts incongruently with its peritectic decomposition occurring at 579 °C. On cooling the melt with composition 2CsCl/1$ThCl_4$ the formation of solid Cs_3ThCl_7 and a solid mixture of Cs_3ThCl_7–$CsThCl_5$ with the eutectic composition is expected. We have found, however,

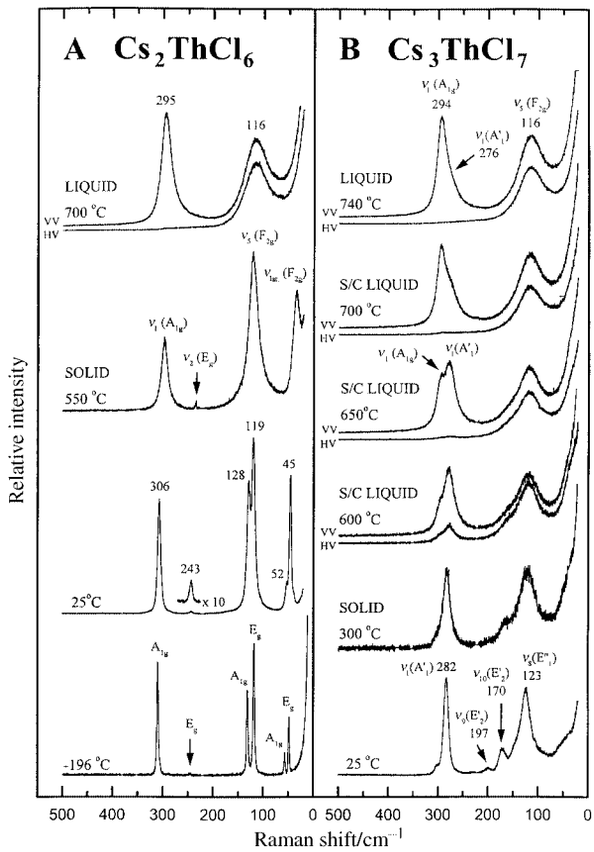

Fig. 1 Raw Raman spectra of: (A) Cs_2ThCl_6 in the solid and liquid phases; the assignments are based on Table 2 and the correlation diagram $O_h \longrightarrow D_{3d}$ given in the text; (B) Cs_3ThCl_7 in the solid, liquid and supercooled liquid phases; the assignments are based on the refs. in Table 3. Spectral conditions: laser line $\lambda_0 = 488.0$ nm, laser power, $w = 100$ mW, spectral slit width (ssw) = 3 cm^{-1}, scan rate 2 cm^{-1} s^{-1}.

that by slow cooling the melt (≈20° per min) we could obtain pure Cs_2ThCl_6 with no impurities due to Cs_3ThCl_7 and $CsThCl_5$. Upon heating the Cs_2ThCl_6 solid the bands participating in the two sets of doublets at frequencies below 150 cm^{-1} (Fig. 2) overlap and form at elevated temperatures two broad well defined bands. In fact, the spectra of the solid at 550 °C exhibit the four peaks Raman pattern characteristic of the cubic $Fm3m(O^5_h)$ symmetry of the Cs_2ZrCl_6[1] and elpasolite[23] crystals. It seems that the amplitude of vibrations of the $ThCl_6^{2-}$ (D_{3d}) octahedra in the trigonal crystal increase with temperature and the species becomes more symmetric yielding gradually an O_h site symmetry and transforming the crystal to cubic. The four modes observed for the high temperature solid are assigned to the three internal modes of the octahedra $\nu_1(A_{1g})$, $\nu_2(E_g)$ and $\nu_5(F_{2g})$. The low frequency lattice mode $\nu_{lat}(F_{2g})$ involves the translatory motion of the Cs^+ cation. The Raman active vibrations of the cubic and the trigonal forms are correlated according to Scheme 1 which agrees with the overlapping of the modes

$$\begin{array}{ccc} O_h & & D_{3d} \\ A_{1g} & \longrightarrow & A_{1g} \\ E_g & \longrightarrow & E_g \\ F_{2g} & \begin{array}{c}\nearrow \\ \searrow\end{array} & \begin{array}{c}A_{1g} \\ E_g\end{array} \end{array}$$

Scheme 1

seen in the temperature dependence spectra (Fig. 1A). It is noteworthy that this is the first time that all the A_{1g} Raman modes of the trigonal $P\bar{3}m1$ (D^3_{3d}) structure for the isostructural Cs_2AnCl_6 crystals have been seen in the spectra. Earlier studies for crystals with An = Th,[24,25] U,[26] Np[27,28] or Pu[29] did not report any splitting of the ν_5 and ν_{lat} modes indicating lower

Table 1 Systems studied and vibrational Raman bands of $ThCl_4$–ACl (A = Li, Na, K or Cs) molten binary mixtures[a] at selected temperatures[b]

$ThCl_4$–LiCl		$ThCl_4$–NaCl		$ThCl_4$–KCl		$ThCl_4$–CsCl	
Mole% $ThCl_4$ (T/°C)	$\tilde{\nu}$/cm^{-1}	Mole% $ThCl_4$ (T/°C)	$\tilde{\nu}$/cm^{-1}	Mole% $ThCl_4$ (T/°C)	$\tilde{\nu}$/cm^{-1}	Mole% $ThCl_4$ (T/°C)	$\tilde{\nu}$/cm^{-1}
						5 (700)	296(297)p,ms[15] 279(280)p,s[40] 155(160)dp,vw,sh 120(128)dp,m
10 (600)	291(292)p,s[45] 272(273)p,m[54] 128(154)dp,m			10 (720)	296(297)p,m[19] 281(282)p,s[46] 160(161)dp,vw 115(131)dp,m	10 (700)	294(295)p,s[18] 277(278)p,ms[37] 157(160)dp,vw,sh 120(126)dp,m
20 (600)	295(297)p,s[45] 279(280)p,m[60] 125(152)dp,m	20 (720)	300(302)p,m[31] 284(285)p,ms[46] (165)dp,vw,sh 118(130)dp,m	20 (700)	297(298)p,m[21] 281(282)p,ms[42] 161(162)dp,vw 115(127)dp,m		
25 (600)	298(299)p,s[43] 280(281)p,m[60] 122(150)dp,m	25 (720)	300(302)p,ms[33] 283(284)p,m[47] 155(165)dp,vw 117(130)dp,m	25 (720)	298(299)p,s[23] 282(283)p,m[43] (≈235)dp,vw 155(160)dp,vw 114(125)dp,m	25 (740)	294(295)p,s[20] 276(277)p,mw[38] (≈230)dp,vw 155(160)dp,vw,sh 116(125)dp,ms
33 (600)	303(305)p,s[44] 282(283)p,m[54] (244)dp,vw 120(147)dp,m	33 (720)	304(306)p,ms[32] 289(290)p,m[41] (≈250)dp,vw 115(130)dp,m	33 (700)	298(299)p,s[26] 283(284),mw[43] 250(250)dp,vw 113(125)dp,ms	33 (700)	295(296)p,s[22] 277(278)p,w,sh[41] (≈245)dp,vw 116(124)dp,ms
						45 (750)	304(305)p,s[30] 264(266)p,mw[35] (230)dp,vw 114(125)dp,m
50 (650)	328(330)p,w,sh 311(312)p,s[49] 282(283)p,m[57] (245)dp,vw 115(144)dp,w	50 (650)	306(308)p,s[40] 279(280)p,m[66] (≈240)dp,vw 110(130)dp,w	50 (700)	305(307)p,s[35] 262(265)p,mw[41] (≈230)dp,vw 112(125)dp,m	50 (700)	305(306)p,s[31] 266(268)p,mw[37] (≈250)dp,vw 112(125)dp,m
77 (730)	330(332)p,s[34] 289(290)p,m[71] (235)dp,vw 110(140)dp,w	75 (720)	325(327)p,s[36] 294(295)p,m[87] (243)dp,vw (≈135)dp,vw	75 (730)	324(325)p,s[34] 291(292)p,m[73] (240)dp,vw (135)dp,vw	75 (700)	321(322)p,s[32] 290(291)p,m[71] (≈235)dp,vw (≈130)dp,vw
		82 (750)	333(335)p,s[30] 295(296)p,m[70] (≈265)dp,vw (≈245)dp,vw (≈135)dp,vw	85 (750)	332(334)p,s[30] 295(296)p,m[76] (244)dp,vw (≈130)dp,vw	87 (750)	332(334)p,s[30] 295(296)p,m[75] (≈240)dp,vw (≈130)dp,vw
100 (800)	339(341)p,s[24] 296(297)p,m[86] (≈260)dp,vw (≈230)dp,vw (≈140)dp,vw					100 (960)	340(342)p,s[25] 301(302)p,m[100]

[a] Numbers in parentheses are values from the reduced spectra; p = polarized, dp = depolarized, s = strong, m = medium, w = weak, v = very, sh = shoulder. Numbers in square brackets are full widths at half maximum (cm^{-1}). [b] Spectra were measured at different temperatures; for temperature effects see text.

distortions of the $AnCl_6^{2-}$ octahedra in these crystals. A possible explanation may lie in the preparation route. Quenching of the melt[30] or rapid precipitation[26] may retain the high symmetry crystal while the gradual cooling used in the present work guarantees the phase transformation to the lower symmetry crystal.

At temperatures a few degrees below 700 °C the solid melts giving a clear solution. In the melt the lattice mode is replaced by a depolarized liquid wing and the ν_1 and ν_5 bands by a polarized and a depolarized band respectively. The liquid bands are broadened, shift to lower frequencies and inverse their intensities relative to the solid. The situation is similar to that observed for the Cs_2ZrCl_6[1] and the elpasolite[23] crystals suggesting that the vibrational modes of the $ThCl_6^{2-}$ in the crystal are transferred to the melt. This is also consistent with analogous studies of the Cs_2AnCl_6 compounds by electronic absorption spectroscopy which indicate that melting for An = U[31] or Np[32] yields octahedrally co-ordinated species. Finally, the octahedral frequencies of molten Cs_2ThCl_6 agree well with those of the same species existing in solutions of $[(C_4H_9)_4N]_2ThCl_6$ in methyl cyanide (ν_1 294, ν_2 255, ν_5 114 cm^{-1}).[33]

Cs_3ThCl_7. There are no crystallographic data for the Cs_3ThCl_7 compound. At ≈90 °C it disproportionates to Cs_2ThCl_6 and CsCl, but quenching from high temperatures yields a stable room temperature solid giving Raman spectral patterns (Fig. 1B) that did not change with time. Despite the lack of crystal structure data it is likely that the compound is isostructural to Na_3ZrF_7[34] which has similar stoichiometry. In the latter crystal the ZrF_7^{3-} species exists as in the case of K_3UF_7,[35] as an isolated complex ion[35] and its Raman spectrum[36] is characterized by three main bands which are attributed to the seven-coordinated species. A comparison of the main Raman frequencies obtained for Na_3ZrF_7 and Cs_3ThCl_7 is given in Table 3. A common scaling factor of ≈2 is valid for all three frequencies on going from Th to Zr. We consider this as an indication that the two compounds contain similar complex ions of the same symmetry and that $ThCl_7^{3-}$ is present in the corresponding salt.

Table 2 Distribution of normal modes of vibration for Cs_2ThCl_6

Space group (no. 164): $P\bar{3}m1(D^3_{3d})$
Molecules per unit cell: 1
Lattice points: 1
Molecules per Bravais cell: 1
Ionic crystal $3N = 27$ normal modes

Correlation diagram

	Point group	Factor group
		D_{3d}
Cs; 2(d)	C_{3v}	
	A_1 →	A_{1g}, A_{2u}
	E →	E_g, E_u
Th; 1(a)	D_{3d}	
	A_{2u} →	A_{2u}
	E_u →	E_u
Cl; 6(i)	C_s	
	A′ →	$2A_{1g}$, $2E_g$, $2A_{2u}$, $2E_u$
	A″ →	A_{2g}, E_g, A_{1u}, E_u

$\Gamma_{3N} = \Gamma_{acoustic} + \Gamma_{translatory}$; $\Gamma_{acoustic} = A_{2u}(IR) + E_u(IR)$, $\Gamma_{translatory} = 3A_{1g}(R) + A_{2g}(i.\alpha) + 4E_g(R) + A_{1u}(i.\alpha) + 3A_{2u}(IR) + 4E_u(IR)$

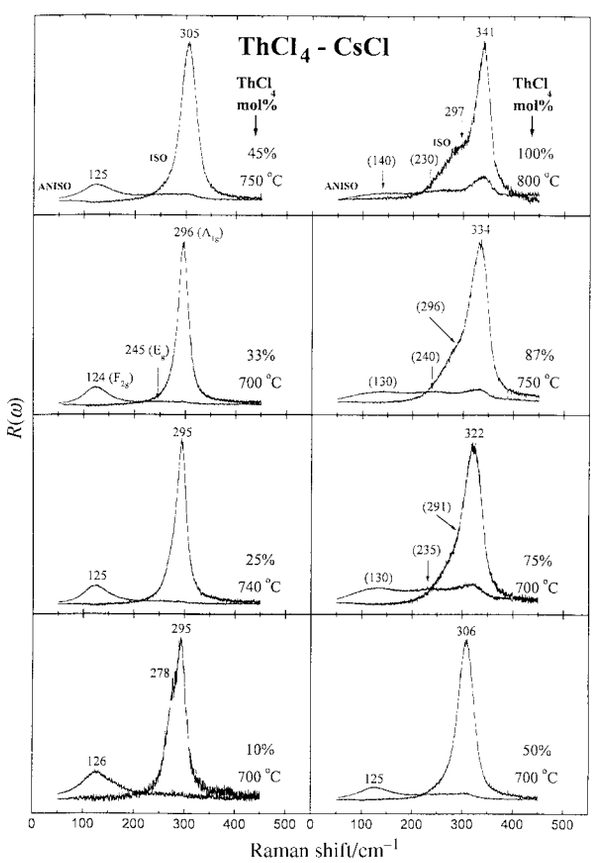

Fig. 2 Reduced isotropic (ISO) and anisotropic (ANISO) spectra of $ThCl_4$–CsCl melt mixtures at different compositions. Spectral conditions as in Fig. 1.

Seven-co-ordinated species are rather scarce and only a few examples are found in the literature. Table 3 lists three of these species that have been characterized by Raman spectroscopy. The assignments assume a D_{5h} (pentagonal bipyramidal) point group symmetry. In all the spectra measured[36,37] the ν_1 polarized mode has the highest intensity while the ν_8 and ν_{10} depolarized modes have weaker but similar intensities. All these observations support the existence of the seven-co-ordinated thorium(IV) species in the solid compound.

Table 3 Main wavenumbers (in cm^{-1}) of seven-co-ordinated compounds

Compound	$\nu_1(A'_1)$	$\nu_{10}(E'_2)$	$\nu_8(E''_1)$	Ref.
Cs_3ThCl_7	282	170	123	This work
Na_3ZrF_7	556	365	250	36
Cs_2BiF_7	536	326	247	37
Cs_2SbF_7	597	391	285	37

The effect of temperature on the Raman spectra of Cs_3ThCl_7 follows the general trends, *i.e.* softening of the vibrational frequencies and broadening of the bands with increasing temperature. This behavior is seen in Fig. 1B by comparing the spectra at 25 and 300 °C. Furthermore, the internal modes of $ThCl_7^{3-}$ predominate at both temperatures. In the melt at 740 °C (Fig. 1B) the overall spectra, apart from a weak shoulder band at ≈280 cm^{-1}, match the pattern of the $ThCl_6^{2-}$ octahedra (Fig. 1A). Presumably a seven- to six-fold co-ordination change occurs upon melting. Slow cooling did not solidify the compound at the mp ≈725 °C and a metastable supercooled liquid was formed at temperatures down to 600 °C. The spectra of this liquid (Fig. 1B) appear to be related to the vibrational frequencies of both the $ThCl_6^{2-}$ and the $ThCl_7^{3-}$ species. With decreasing temperature the $\nu_1(A_{1g})$ breathing mode of the octahedra at ≈295 cm^{-1} loses intensity in favor of the $\nu_1(A'_1)$ symmetric axial stretching of $ThCl_7^{3-}$ at ≈280 cm^{-1}. The former and the latter species predominate at 740 and 600 °C respectively. Thus, the temperature evolution of the liquid/supercooled liquid spectra suggest that an equilibrium of the type (1) might take

$$ThCl_6^{2-} + Cl^- \rightleftharpoons ThCl_7^{3-} \quad (1)$$

place in this melt mixture. The concentration and temperature dependence of the spectra discussed below shows that this is indeed the case.

$ThCl_6^{2-}$ and $ThCl_7^{3-}$ in melt mixtures rich in alkali-metal chloride

The spectra of molten $ThCl_4$–ACl (A = Li, Na, K or Cs) at $X_{ThCl_4} \approx 0.33$ are characterized by two main bands and are similar to those of the Cs_2ThCl_6 melt. This suggests that at 33% composition the $ThCl_6^{2-}$ octahedra are the predominant species in all these melts. The frequencies of the two bands $\nu_1(A_{1g}) \approx 295$ cm^{-1} and $\nu_5(F_{2g}) \approx 116$ cm^{-1} are not affected by the counter cation (A^+); this is in contrast to other MCl_n–ACl (M = trivalent or divalent cation)[2] where an increasing small red shift of the metal–halide stretching frequency has been observed in the sequence CsCl to LiCl. Presumably due to the high ionic potential of the thorium(IV) cation and its strong acceptor character towards Cl^-, the counter cation does not affect the Th–Cl bonding within the octahedra. However, the counter cation influences the half width of the ν_1 band which is ≈22 cm^{-1} for the CsCl melt and increases to ≈45 cm^{-1} for the LiCl melt. This suggests that the lifetime of the $ThCl_6^{2-}$ configuration increases with decreasing ionic potential of the counter cation.

At compositions $X_{ThCl_4} < 0.33$ the $ThCl_6^{2-}$ spectra do not change drastically. The position of the ν_1 and ν_5 bands remains approximately constant for all these melts. The formation of the $ThCl_6^{2-}$ species is further supported by measurements of the normalized (per mol of $ThCl_4$) relative Raman intensity of the 295 cm^{-1} band which is found to remain constant at all compositions studied.

However, the symmetric gaussian shape of the ν_1 band (Fig. 2) changes with decreasing $ThCl_4$ mole fraction. A shoulder

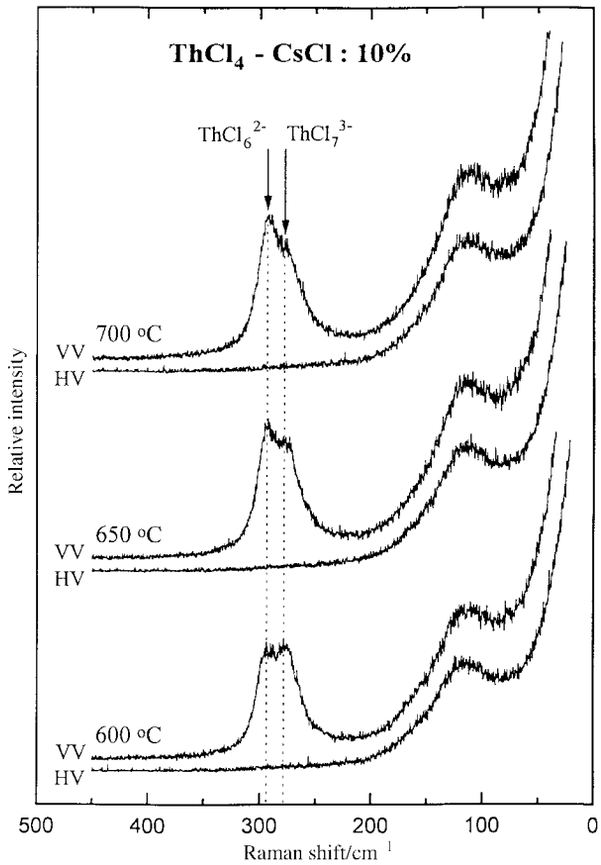

Fig. 3 Temperature dependence of the raw Raman spectra for the $ThCl_4$–CsCl (10:90) melt mixtures. Spectral conditions as in Fig. 1.

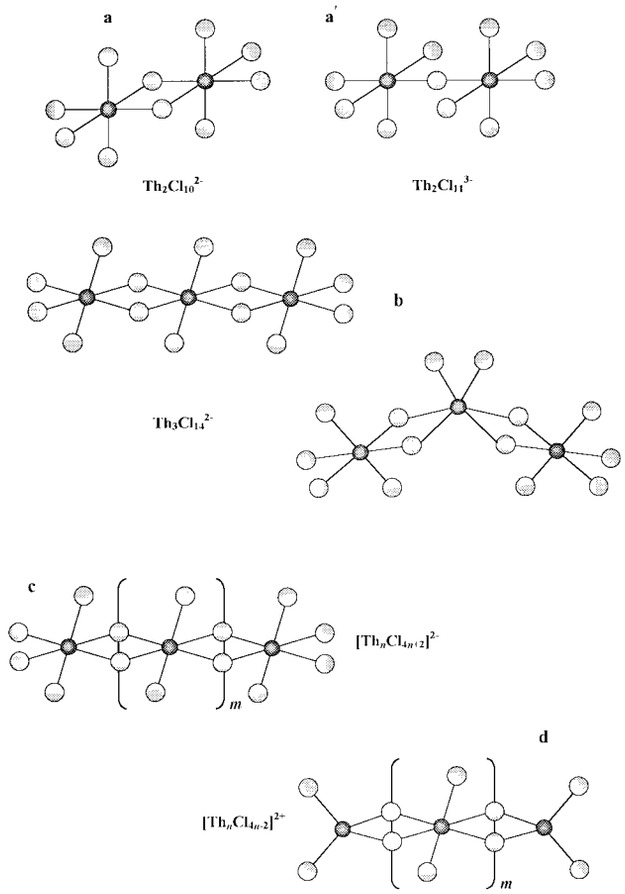

Fig. 4 Molecular models of thorium(IV) chloride species.

band gradually appears in the spectra and at compositions dilute in $ThCl_4$ the octahedral $\nu_1(A_{1g})$ band at 295 cm^{-1} acquires a partner band at 280 cm^{-1}. The band is well resolved in the CsCl system (Figs. 2 and 3) at $X_{ThCl_4} \approx 0.1$ but loses intensity and remains as a shoulder band in the binaries with KCl, NaCl and LiCl. The frequency of the new band is at lower energy than that of $ThCl_6^{2-}$ indicating a species with co-ordination higher than six. Based on the previous discussion regarding the Cs_3ThCl_7 solid and the data in Table 3, we assign the new band to the $\nu_1(A'_1)$ mode of the $ThCl_7^{3-}$ species.

Spectra measured for the $ThCl_4$–CsCl melts with $X_{ThCl_4} = 0.1$ and 0.05 clearly resolve the $\nu_1(A_{1g})$ and $\nu_1(A'_1)$ stretching frequencies of the $ThCl_6^{2-}$ and $ThCl_7^{3-}$ species respectively. Furthermore, the changes of relative intensities with temperature, as shown in Fig. 3, suggest that equilibrium (1) is established in these melts.

The seven-co-ordinated species is favored at lower temperatures and in melts having counter cations with low ionic potential. Accurate relative intensity measurements of the $\nu_1(A_{1g})$ and $\nu_1(A'_1)$ bands were used as before [19b] to calculate the enthalpy of the above ionic equilibria; a value of $\Delta H \approx 8$ kcal mol^{-1} was obtained.

Associated octahedral thorium chloride ions at composition $X_{ThCl_4} > 0.33$

The systematics of the Raman spectra for the $ThCl_4$–ACl mixtures are depicted in Fig. 2 for the CsCl melts. For all other alkali-metal halides the spectra are very similar with respect to the number and the position of the bands. Differences have been noted in the band half widths which increased in the sequence from CsCl to LiCl. Furthermore, as discussed above, differences exist in the very dilute $ThCl_4$ mixtures where the $ThCl_7^{3-}$ band is better resolved in the CsCl than in the other three alkali-metal chloride melts. The calculation and use of the reduced isotropic and anisotropic representation of the spectra shown in Fig. 2 has certain advantages as discussed in ref. 3, one being the ability better to resolve and distinguish overlapping polarized and depolarized bands. This can easily be seen for the 33 mol% mixture (Fig. 2) where, apart from the A_{1g} and F_{2g} band, the position of the weak depolarized E_g band can be estimated.

The gradual increase of the $ThCl_4$ mole fraction at compositions above 33% yields the following spectral changes (Fig. 2): (a) the ν_1 octahedral band at 295 cm^{-1} shifts continuously to higher energies reaching a value of 341 cm^{-1} in pure $ThCl_4$; (b) a new polarized band at ≈290 cm^{-1} grows as a shoulder on the strong polarized band; (c) the intensity of the 125 cm^{-1} depolarized band diminishes with increasing $ThCl_4$ content and a weak depolarized band at ≈250 cm^{-1} appears; (d) a new depolarized band also grows continuously under the strong polarized band reaching its maximum intensity in the spectra of pure $ThCl_4$. Furthermore the spectra were found to be rather insensitive to temperature variations with the exception of the expected band broadening with increasing temperature. All the above changes suggest that continuous structural changes occur in the melt mixtures and this to some extent is opposite to what was observed in the $ZrCl_4$–CsCl [1] systems where different zirconium chloride ions in equilibria could account for the spectral changes and their temperature dependence.

One possible way to account for the continuous spectral changes is to allow an extended linkage of $ThCl_6^{2-}$ octahedra in the melt. Thus, the addition of $ThCl_4$ to the 33 mol% mixture containing the $ThCl_6^{2-}$ octahedra leads to the formation of structural units having two octahedra linked by a corner or an edge (Fig. 4a,a′). Such a linkage continues up to 50% where the maximum single edge sharing is anticipated leading most probably to the formation of $Th_2Cl_{10}^{2-}$. Owing to the bridging, the Th–Cl_t terminal frequency is expected at higher energy than that of the free $ThCl_6^{2-}$ and this accounts for the shift of the

strong polarized band on going from the 33 to the 50 mol% mixture. Raman spectra measured for the 50 mol% mixture at 520, 600 and 700 °C were identical showing a pronounced stability of the melt. In this respect it is interesting that vapor pressure measurements over molten $ThCl_4$–ACl mixtures show that the predominant vapor species are $ThCl_4$(g), ACl(g) and complexes with the general stoichiometry $AThCl_5$(g).[14] Such a behavior supports the stabilization of the 50 : 50 mixture with associated thorium chloride species.

Further increase of the $ThCl_4$ mol fraction may extend the linkage to form a three edge-sharing octahedral species $Th_3Cl_{14}^{2-}$ (Fig. 4b,b′) having its maximum concentration at $X_{ThCl_4} \approx 0.6$. The $Th_3Cl_{14}^{2-}$ species is the first of a series of chains formed by edge-sharing octahedra with the general formula $[Th(Cl_t)_4[Th(Cl_t)_2(Cl_b)_4]_mTh(Cl_t)_4]^{2-}$ (Fig. 4c). The middle Th atoms in this structure are surrounded by four bridging (Cl_b) and two terminal (Cl_t) chlorides. Most probably at $X_{ThCl_4} > 0.5$ the Th–Cl_b vibrations initiate the appearance of the second polarized band ($\nu_b \approx 295$ cm^{-1}) while the Th–Cl_t vibration having energy higher than that of $Th_2Cl_{10}^{2-}$ is responsible for the further blue shift of the strong polarized band.

The proposed chain octahedral species are doubly charged having as counter cations the A^+. Thus, to an extent the structure is compatible with the ionic conductivity of these mixtures under the assumption that the value of m is small, *i.e.* that the chain ions are oligomers. However, discrepancies may occur in mixtures very rich in $ThCl_4$ and in pure $ThCl_4$ melts where a deficiency of cations is expected. This problem is examined in the following section.

Finally it should be noted that there are two possible ways of edge bridging the octahedra: (a) with the opposite edges of the equatorial chlorines leading to linear chains or (b) with adjacent edges leading to zigzag chains (as in Fig. 4b). Octahedra linked by corner sharing cannot be excluded especially at $X_{ThCl_4} < 0.4$ while the formation of face sharing bioctahedral $Th_2Cl_9^-$ (found in the $ZrCl_4$ mixtures) is rather improbable due to the high repulsive potential between the thorium(IV) cations.

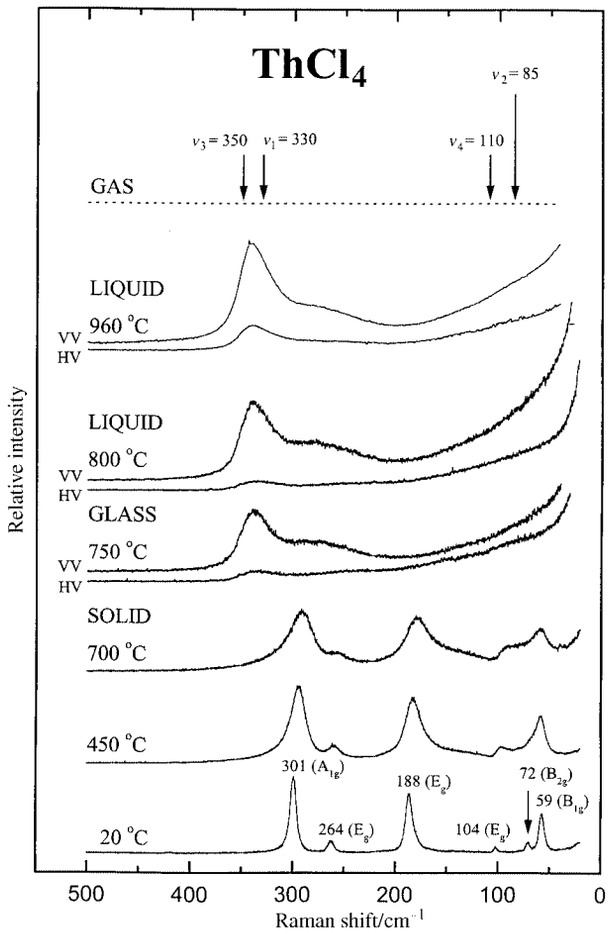

Fig. 5 Raw Raman spectra of $ThCl_4$ in the solid, liquid and glassy states. Upper part indicates the estimated vibrational frequencies of gaseous $ThCl_4$. Spectral conditions as in Fig. 1 with the exception of liquid spectra at 960 °C where $\lambda_0 = 488.0$ nm, $w = 400$ mW, ssw = 5 cm^{-1}, integration time = 5 s.

The structure of molten and glassy $ThCl_4$

Solid thorium tetrachloride is a polymorphic material.[38,39] The low temperature α form is tetragonal $I4_1/a$ (C_{4h}^6) with the Th atom in S_4 site symmetry. The β form is stable above 405 °C, has a tetragonal space symmetry $I4_1/amd$ (D_{4h}^{19}) with the Th atom in a D_{2d} site symmetry. Quenching of the melt or the high temperature solid stabilizes the β form at ambient temperatures. Other crystal modifications at temperatures below 90 K have also been reported.[40] In both tetragonal structures each Th atom is surrounded by a dodecahedron of eight chlorine atoms which are shared between neighboring Th atoms. Single crystal Raman spectra of the β form have been obtained and the expected vibrational modes have been successfully assigned.[40] In Fig. 5 we present the Raman spectra of polycrystalline β-$ThCl_4$ at different temperatures; the assignments are taken from ref. 40.

In the vapor phase thorium chloride forms mainly $ThCl_4$ monomers with a tetrahedral symmetry.[41–44] Our attempts to obtain Raman spectra of gaseous $ThCl_4$ were unsuccessful due to the extreme and fast corrosion of the cell walls at high temperatures. However, by combining IR matrix isolation[45] and gaseous[46] spectra with thermodynamic calculations[43,44] and electron diffraction[42] and by scaling to the vibrational frequencies of gaseous UCl_4,[45,47] $ZrCl_4$[1] and $HfCl_4$[6] molecules we could estimate the Raman frequencies for the $ThCl_4$ gas. The values of these frequencies are marked on the top of Fig. 5.

In the same Fig. 5 we present the spectra of molten and glassy $ThCl_4$. The spectra were recorded in the sequence 800 °C (liquid) ⟶ 750 °C (glass) ⟶ 600–580 °C (glass crystallizes) ⟶ 700 °C (solid) ⟶ 450 °C (solid) ⟶ 20 °C (solid). As before with increasing temperature the solid bands increase their width and in general exhibit a small frequency red-shift. Upon melting drastic changes occur in the spectra. The highest strong band of the high temperature solid at ≈293 cm^{-1} (A_{1g}) is replaced in the liquid by the 340 cm^{-1} strong polarized band while all the other solid bands disappear in the liquid wing. No correlation between the solid and liquid spectra can be established. The ≈50 cm^{-1} difference between the A_{1g} solid mode and the strong polarized liquid band suggests that the eightfold co-ordination of thorium(IV) in the solid decreases in the melt. Obviously the liquid spectra are more related to the continuous spectral and structural changes occurring in the $ThCl_4$–ACl melt mixtures (Fig. 2) than the solid structure.

Thorium(IV) chloride melts at 771 °C[7,8,48] forming a rather fluid liquid with a molar volume expansion. From data in refs. 5, 39 and 49 an increase in molar volume upon melting between 10 and 27% can be calculated. Despite the contradictory liquid density data,[5,49] molten $ThCl_4$ exhibits a negligible further expansion with increasing temperature, ruling out drastic structural changes and excluding a monomer–dimer equilibrium similar to that found for $ZrCl_4$. In support of this are the similarities of the relative intensities observed in the liquid and the glass spectra shown in Fig. 5. Finally the electrical conductivity of $ThCl_4$ ($\sigma_{810\,°C} \approx 0.6\ \Omega^{-1}$ cm^{-1}) points to an ionic melt with some kind of order.[5]

The observed 341 cm^{-1} band of the melt is close to the predicted $\nu_1(A_1) \approx 330$ cm^{-1} breathing mode of the gaseous tetrahedral molecule and thus the (partial) presence of such molecules in the $ThCl_4$ melts cannot be excluded. Molten $ZrCl_4$ is mainly molecular and this is reflected in both its Raman spectra and its (molecular) electrical conductivity.[1] In contrast molten

$ThCl_4$ should have a structure that also allows the presence of ions so as to justify its ionic conductivity. If we assume that the model with the doubly negative charged chains proposed in the previous section for molten mixtures rich in $ThCl_4$ is applicable to some extent to pure $ThCl_4$, then the mechanism should create oppositely charged species having vibrational frequencies that can be verified by the Raman spectra. One such mechanism, compatible with the continuous structural changes in the melt mixtures and the proposed oligomer anion (Fig. 4c), could involve a self ionization scheme of the type (2).

$$n\mathrm{ThCl_4} \rightleftharpoons \tfrac{1}{2}[\mathrm{Th}_n\mathrm{Cl}_{4n-2}]^{2+} + \tfrac{1}{2}[\mathrm{Th}_n\mathrm{Cl}_{4n+2}]^{2-} \quad (2)$$

The structure of the doubly charged anion is the same as before (Fig. 4c) while that of the doubly charged cation is similar to that of the anion but having two Th atoms at the end of the chain in a fourfold co-ordination (Fig. 4d) instead of the sixfold proposed for the anion. The terminal frequency of the fourfold co-ordinated Th atom in the cation is expected at higher energies than the ν_1 mode of gaseous $ThCl_4$; this agrees with the blue-shift seen in the frequencies on going from the gas to the melt. Furthermore, as was pointed out in the previous section, the terminal frequency of the sixfold co-ordinated Th atom at the end or the middle of the chain is expected at energies higher than that of the isolated $ThCl_6^{2-}$ octahedra. Thus, the envelope of the 340 cm^{-1} band of the melt covers all the terminal Th–Cl_t frequencies arising from both the four- and the six-fold co-ordinated thorium in the cation plus the sixfold terminal frequencies of the anion. In turn, the envelope of the broad band at 295 cm^{-1} covers all the bridging frequencies for both species.

A similar ionization scheme to the above has recently been proposed for molten iron(III) chloride.[50] Neutron diffraction studies[51] and detailed Raman spectroscopic measurements converge in supporting the self-ionization model and account for the ionic conductivity of this melt.[52] As in the case of iron(III) chloride the size of the chain thorium ions, formed according to reaction (2), should be small in order to justify both the electrical conductivity and the fluidity of molten $ThCl_4$. With reference to Fig. 4c/4d we anticipate that the chain length is limited to $m < 3$. For the cation (Fig. 4d) the value of $m = 0$ is rather unlikely because of the strong Th–Th repulsions within the bitetrahedral $[Th_2Cl_6]^{2+}$ while for the anion (Fig. 4c) $m \geq 1$.

In separate experiments we have measured by fast Raman techniques the spectra of the liquid up to 960 °C. The spectral pattern did not change, but it was found that with increasing temperature the intensity of the 341 cm^{-1} band is slightly enhanced relative to that of the 295 cm^{-1} band. This behavior is seen in the upper two spectra of Fig. 5 and is compatible with both the above assignment of the 295 and 341 cm^{-1} bands and the proposed structural model for molten $ThCl_4$. In other words, increasing temperature induces breaking of the bridged bonds and either shifts reaction (2) to the left or/and lowers the m values of the anions/cations.

Slow cooling of molten $ThCl_4$ to temperatures below melting gave a transparent material which started crystallizing near 600 °C. Visually the material had no fluidity and thus we assume that this supercooled melt was in the glassy state. Similar supercooling had previously been detected by DTA down to 750 °C. Supercooling was also reported in the $ThCl_4$–LiCl and $ThCl_4$–NaCl phase diagrams,[7] whereas thin film glass formation has been found in the ternary $ThCl_4$–NaCl–KCl phase diagram.[53] Throughout the liquid to glass transformation the Raman spectra did not change drastically indicating structural similarities for both phases. However, a small increase in the intensity ratio of the 295 cm^{-1}/341 cm^{-1} bands occurs in the glass relative to the melt which is in the expected direction from the temperature variation of the liquid spectra. This again infers somewhat more extended bridging in the glass, *i.e.* longer chains/higher average m values (Fig. 4c,d). On going from the high temperature melt (at 960 °C) to the glass the overall changes of the intensity ratio are rather small indicating that the equilibrium constant of reaction (2) is not very sensitive to temperature and that the composition (the m value) of the two ions participating in the reaction does not change much. Thus, it is more likely that the equilibrium is well shifted to the right (*i.e.* strong self ionization of $ThCl_4$) which implies that the average co-ordination of Th^{IV} in the melt is closer to six than to four. In this respect the determination of the average co-ordination number of thorium(IV) in molten $ThCl_4$ by neutron diffraction of isotopically enriched samples would be elucidating.

References

1 G. M. Photiadis and G. N. Papatheodorou, *J. Chem. Soc.*, *Dalton Trans.*, 1998, 981.
2 M. H. Brooker and G. N. Papatheodorou, in *Advances in Molten Salt Chemistry*, eds. G. Mamantov and G. B. Mamantov, Elsevier, New York, 1983, vol. 5, p. 27.
3 G. M. Photiadis, B. Borresen and G. N. Papatheodorou, *J. Chem. Soc.*, *Faraday Trans.*, 1998, 2605 and refs. therein.
4 R. Oyamada, *J. Phys. Soc. Jpn.*, 1972, **32**, 1044.
5 S. Yoshida, R. Oyamada and T. Kuroda, *Denki Kagaku*, 1968, **36**, 297.
6 R. J. H. Clark, B. K. Hunter and D. M. Rippon, *Inorg. Chem.*, 1972, **11**, 56.
7 V. M. Vdovenko, A. Y. Gershanovich and I. G. Suglobova, *Radiokhimiya*, 1974, **16**, 886; *Sov. Radiochem.* (*Engl. Transl.*), 1974, **16**, 863.
8 A. Y. Gershanovich and I. G. Suglobova, *Radiokhimiya*, 1980, **22**, 265; *Sov. Radiochem.* (*Engl. Transl.*), 1980, **22**, 201.
9 S. Yoshida, T. Ayano and T. Kuroda, *Denki Kagaku*, 1973, **41**, 427.
10 R. Oyamada, S. Yoshida and T. Kuroda, *Denki Kagaku Oyobi Kogyo Butsuri Kagaku*, 1969, **37**, 417; *Chem. Abstr.*, 71, 95474k.
11 S. Yoshida, S. Kaji and K. Kawamura, *Denki Kagaku Oyobi Kogyo Butsuri Kagaku*, 1975, **43**, 195; *Chem. Abstr.*, 83, 183499a.
12 P. J. Tumidajski and S. N. Flengas, *Can. J. Chem.*, 1991, **69**, 462.
13 A. Kolotii and Y. K. Delimarskii, *Zh. Neorg. Khim.*, 1963, **8**, 82.
14 M. V. Smirnov and V. Y. Kudyakov, *Electrochim. Acta*, 1984, **29**, 63.
15 S. Yoshida, R. Oyamada and K. Kawamura, *Bull. Chem. Soc. Jpn.*, 1978, **51**, 25.
16 R. Oyamada and S. Yoshida, *J. Phys. Soc. Jpn.*, 1975, **38**, 1786.
17 L. M. Toth and G. E. Boyd, *J. Phys. Chem.*, 1973, **77**, 2654.
18 J. L. Willit, W. E. Miller and J. E. Battles, *J. Nucl. Mater.*, 1992, **195**, 229.
19 (*a*) V. Dracopoulos and G. N. Papatheodorou, *Proc. XI Symposium on Molten Salts*, *ECS*, 1998, **98-11**, 545; (*b*) S. Boghosian and G. N. Papatheodorou, *J. Phys. Chem.*, 1989, **93**, 415.
20 G. M. Photiadis, Thesis (in Greek), Chemical Engineering Department, University of Patras, 1999, containing spectra and tables with English labellings.
21 S. Siegel, *Acta Crystallogr.*, 1956, **9**, 827.
22 D. Brown, *Halides of the Lanthanides and Actinides*, Wiley, London, 1968, p. 146.
23 G. N. Papatheodorou, *J. Chem. Phys.*, 1977, **66**, 2893.
24 A. D. Westland and M. T. H. Tarafder, *Can. J. Chem.*, 1983, **61**, 1573.
25 D. Brown, B. Whittaker and P. E. Lidster, *U.K. At. Energy Res. Establ.*, *Rep.*, AERE-R8035, 1975, 16 pp.; *Chem. Abstr.*, 83, 155028c.
26 J. Shamir and A. Silberstein, *J. Inorg. Nucl. Chem.*, 1975, **37**, 1173.
27 B. W. Berringer, J. B. Gruber, T. M. Loehr and G. P. O'Leavy, *Bull. Am. Phys. Soc.*, 1970, **15**, 1602.
28 B. W. Berringer, J. B. Gruber, T. M. Loehr and G. P. O'Leary, *J. Chem. Phys.*, 1971, **55**, 4608.
29 L. R. Morrs and T. Fujino, *J. Solid State Chem.*, 1988, **72**, 338.
30 T. Schleid, G. Meyer and L. R. Morss, *J. Less-Common Met.*, 1987, **132**, 69.
31 J. R. Morrey, *Inorg. Chem.*, 1963, **2**, 163.
32 Y. A. Barbanel, V. P. Kotlin, V. V. Kolin and C. P. Chudnovskaya, *Radiokhimiya*, 1975, **17**, 929; *Sov. Radiochem.* (*Engl. Transl.*), 1975, **17**, 812.
33 L. A. Woodward and M. J. Ware, *Spectrochim. Acta*, *Part A*, 1968, **24**, 921.
34 L. A. Harris, *Acta Crystallogr.*, 1959, **12**, 172.
35 W. H. Zachariasen, *Acta Crystallogr.*, 1954, **7**, 792.
36 L. M. Toth, A. S. Quist and G. E. Boyd, *J. Phys. Chem.*, 1973, **77**, 1384.

37 G. W. Drake, D. A. Dixon, J. A. Sheehy, J. A. Boatz and K. O. Christe, *J. Am. Chem. Soc.*, 1998, **120**, 8392.
38 J. T. Mason, M. C. Jha and P. Chiotti, *J. Less-Common Met.*, 1974, **34**, 143.
39 K. Mucker, G. S. Smith, Q. Johnson and R. E. Elson, *Acta Crystallogr.*, *Sect. B*, 1969, **25**, 2362.
40 S. Hubert, P. Delamoye, S. Lefrant, M. Lepostollec and M. Hussonnois, *J. Solid State Chem.*, 1981, **36**, 36.
41 Y. S. Ezhov, P. A. Akishin and N. G. Rambidi, *Zh. Strukt. Khim.*, 1969, **10**, 763.
42 V. I. Bazhanov, Y. S. Ezhov, S. A. Komarov and V. G. Sevast'yanov, *Zh. Strukt. Khim.*, 1990, **31**, 153.
43 D. L. Hildenbrand, K. H. Lau and R. D. Brittain, *J. Chem. Phys.*, 1991, **94**, 8270.
44 K. H. Lau and D. L. Hildenbrand, *J. Chem. Phys.*, 1990, **92**, 6124.
45 I. R. Beattie, P. J. Jones, K. R. Millington and A. D. Willson, *J. Chem. Soc.*, *Dalton Trans.*, 1988, 2759.
46 A. Buchler, J. B. Berkowitz-Mattuck and D. H. Dugre, *J. Chem. Phys.*, 1961, **34**, 2202.
47 J. B. Gruber and H. G. Hecht, *J. Chem. Phys.*, 1973, **59**, 1713.
48 P. Chiotti, J. E. Fuller, C. H. Dock and M. C. Jha, *J. Less-Common. Met.*, 1973, **31**, 365.
49 V. N. Desyatnik and N. M. Emel'yanov, *Zh. Prikl. Khim.*, 1975, **48**, 1382; *J. Appl. Chem. USSR*, 1975, **48**, 1434.
50 G. N. Papatheodorou and G. A. Voyiatzis, *Chem. Phys. Lett.*, 1999, **303**, 151.
51 D. L. Price, M. L. Saboungi, J. Wang, S. C. Moss and R. L. Leheny, *Phys. Rev. B*, 1998, **57**, 10496.
52 H. A. Andreasen, N. J. Bjerrum and N. H. Hansen, *J. Chem. Eng. Data*, 1980, **25**, 236.
53 H. Hu and J. D. Mackenzie, *J. Non-Cryst. Solids*, 1982, **51**, 269.

Paper 9/05065E